

## CLLOUD MAPPING USING GROUND-BASED IMAGERS

**Gabriela SEIZ, Manos BALTSAVIAS**  
Swiss Federal Institute of Technology, Zurich  
Institute of Geodesy and Photogrammetry  
(gseiz, manos)@geod.baug.ethz.ch

**KEY WORDS:** Camera Calibration, Global Change, Image Matching, Sky Imagers, Sensor Orientation, Clouds.

### ABSTRACT

A ground-based sky imager system consisting of two commercial digital CCD cameras with wide-angle lenses has been developed. The system can be used to derive various macroscopic cloud parameters: cloud amount, cloud-base heights and cloud-base wind (for every visible cloud layer). The method to calculate a DSM of the cloud-base is presented. It includes the precise determination of the interior and exterior orientation of the cameras, which have been carried out with a close-range photogrammetric testfield, stars and special airplane flights (equipped with DGPS). The data acquisition took place in the Upper Rhine Valley, Switzerland in October 1999 and was part of the SOP (Special Observing Period) campaign of the programme MAP (Mesoscale Alpine Programme). Cloud-base heights have been derived automatically using commercial digital photogrammetric systems and own software. A comparison of the results with other operational and MAP-only measurements/observations is shown. Finally, a case study of coincident ground- and satellite-based retrieval of cloud-base/cloud-top height for a vertically thin cirrus cloud formation is presented.

### 1 INTRODUCTION

The relative placement and character of clouds can have a strong impact on both the total incoming radiation at the surface and the reflected radiation above the cloud field. Cloud-base height (CBH) is a dominant factor in determining the infrared radiative properties of clouds (Allmen and Kegelmeyer, 1996). However, cloud-base heights are not well known from the existing observation networks. Cloud macroscopic properties – mainly cloud cover, cloud depth and cloud-base height – are normally eye-observed at the climate stations of the national networks. Mainly at airports, ceilometers are in operational use to measure cloud parameters automatically and continuously in addition to the eye-observations. It is well recognized today that the infrequent, spatially not equally distributed, subjective and too sparse point observations of clouds do not satisfy the needs of Numerical Weather Prediction (NWP) and Global Climate Models (GCM). Ground-based imagers are one possible system to fulfil some of the necessities described above. Practical fieldwork with other whole-sky imager systems (Shields et al., 1999) has been performed at various ARM (Atmospheric Radiation Measurement) Program sites (Stokes and Schwartz, 1994). The data of a ground-based imager system has the further advantage of being more easily interpretable compared to point measurements of cloud-base from ceilometers, lidars or radars.

### 2 MEASURE SITE AND EXPERIMENTAL SETUP

The data acquisition took place during the Special Observing Period (SOP) of the programme MAP (Mesoscale Alpine Programme). MAP is an international research initiative devoted to the study of atmospheric and hydrological processes over mountainous terrain. It aims towards expanding our knowledge of weather and climate over complex topography (MAP Science Plan, 1998). The SOP measurements were focused on three target areas (MAP Implementation Plan, 1999): “Lago Maggiore”(CH/I), “Rhine Valley”(CH) and “Brennerpass/ Wipp Valley”(A). The SOP period lasted from September, 7 to November, 15, 1999. At “Foehn” events North of the Alps (Rhine Valley, Brennerpass) or at heavy precipitation events South of the Alps, Intensive Observation Periods (IOP) of 2-5 days were defined.

Our two camera locations were situated at Mels within the target area “Rhine Valley”, Switzerland (Fig. 9), and were separated by 850 meters horizontally. The relatively short distance was chosen to be able to stereo analyse also low clouds. The choice of an appropriate base length for cloud mapping is difficult because of the wide height range of clouds (up to 15 km). For future operational applications of a stereo cloud mapping system, the use of a dynamic distance between the two cameras with respect to the actual cloud height range should be evaluated. This adaptation of

the base length would optimize the base-to-height ratio especially for high cloud situations. The two locations were visible from each other; the baseline direction was parallel to the valley direction, from NW to SE.

Each camera system consists of a KODAK DCS460 colour digital CCD camera (Fig. 1) connected via SCSI interface to a laptop with precise time information (GPS receiver or radio clock). The shutter release is controlled by a C++ program from the laptop, with use of the KODAK PDC-SDK library. The camera is mounted on an adapted theodolite tripod which allows precise horizontal adjustment of the camera with levelling screws and with the use of an electronic levelling instrument on the lens. The approximate adjustment of the azimuth parallel to the baseline has been done – due to the visibility of the other camera – with a small telescope. The tripod has a moving sun occultator device (which can be used against image blooming caused by the sun) and a small heating device to stabilise the camera against temperature and humidity variations during longer image series and during the night image acquisition.

Two types of wide-angle lenses were used, a Nikon 18mm with a nominal viewing angle of  $100^\circ$  and a Nikon 8mm fisheye with a viewing angle of  $180^\circ$ . The results presented in this paper concentrate on the images taken with the 18mm lenses.

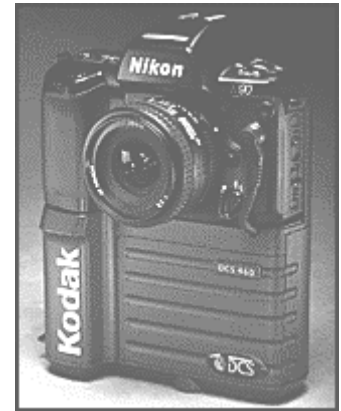


Figure 1. KODAK DCS460c

### 3 KODAK DCS460 SENSOR



Figure 2. Bayer colour filter

The camera's CCD array is a KAF-6300 with  $3072 \times 2048$  pixels, each  $9 \times 9 \mu\text{m}^2$ , with a Bayer colour filter (Bayer, 1976) (Fig. 2). In the KODAK image processing software, the 6 rows and columns around the edge of the array are discarded. The RGB values (8- or 12-bit per colour) of the remaining  $3060 \times 2036$  pixels are calculated with KODAK proprietary Active Interpolation algorithm from the originally 8-bit red, green and blue filter values (Adams et al., 1998). As the colour interpolation algorithm tends to distort edges and creates artifacts, an own interpolation may be necessary for certain applications. For the matching of cloud points, there was no relevant difference between the image with active interpolation and an image generated from the raw 8-bit values.

The dark current noise of this sensor is quite substantial and influences especially the long exposure time night images which are used for exterior orientation with stars (see Section 4.3). Therefore, images with the lens cap closed were taken at various exposure times between 0.002 and 240 seconds for each camera to analyze the dark current noise. It was shown that the flat field is camera-dependant, spatially variable, temporally stable and increases with longer exposure times.

## 4 CAMERA CALIBRATION

### 4.1 Inner Orientation

The inner orientation parameters are determined with a close-range photogrammetric reference field of  $4.2 \times 2 \times 1.2$  m at our Institute (Fig. 3). The 3-D coordinates of 77 small signalized points and 20 coded points on the reference field had been measured using a theodolite system with an accuracy of 0.04mm. This accuracy is similar to previous measurements of the testfield (Beyer, 1992). The remeasurement of the points was necessary due to possible changes from the construction work in the building.

For each camera, 15 images were taken: from 5 camera stations (left high, left low, center, right high, right low) at three different roll angles ( $-90^\circ$ ,  $0^\circ$ ,  $+90^\circ$ ). Before the calibration process, the CCD chip was fixed with respect to the camera-back so that no movement of the chip occurs during the calibration and during the fieldwork. The instability of the Kodak DCS CCD arrays due to the spring mounting (mounting of the chip only at one side against shock influence) is described in (Shortis et al., 1998). A second testfield calibration of both cameras after the measurement campaign will be evaluated to estimate the stability of the calibration and of the CCD chip with the additional fixing.



Figure 3. Reference field

The camera model parameters were calculated simultaneously with camera orientation data and 3-D object point coordinates, employing a self-calibrating bundle adjustment. Ten additional parameters were used to model systematic errors (Brown, 1971): three parameters of interior orientation (focal length offset  $d_c$ , principal point coordinate offsets  $d_{x_p}$  and  $d_{y_p}$ , five parameters modelling radial and decentering lens distortion (radial coefficients  $k_1$ ,  $k_2$ ,  $k_3$ ; decentering coefficients  $p_1$ ,  $p_2$ ) and two parameters for a differential scale factor and a correction of the non-orthogonality of the image coordinate axes (Beyer, 1992). Table 1 lists the result of the calibration for both cameras. The differential scale factor, the non-orthogonality factor and some of the lens distortion coefficients proved to be insignificant.

	$c$ [mm]	$x_p$ [mm]	$y_p$ [mm]	$k_1$ [mm <sup>-2</sup> ]	$k_2$ [mm <sup>-4</sup> ]	$p_1$ [mm <sup>-1</sup> ]
Zeughaus, Mels	18.641453 $\pm 1.338e-03$	0.305271 $\pm 6.241e-04$	-0.269040 $\pm 1.766e-03$	-2.983e-04 $\pm 7.614e-07$	5.940e-07 $\pm 4.587e-09$	2.679e-05 $\pm 1.576e-06$
Wiftech AG, Mels	18.516242 $\pm 1.064e-03$	0.279594 $\pm 4.690e-04$	0.069326 $\pm 1.595e-03$	-2.370e-04 $\pm 7.990e-07$	5.223e-07 $\pm 5.218e-09$	-7.414e-06 $\pm 1.286e-06$

Table 1. Additional parameters and their standard deviation as determined from the testfield calibration.

## 4.2 Exterior Orientation from Calibration Flight

A previously calculated flight pattern was flown by the KingAir of the Swiss Army. The flight lines were parallel to the baseline of the two cameras. The highest line was at 4000m above ground, because of air restrictions, the lowest line at 1000m above ground. The lines were along the left and right edge of the images and along the middle.

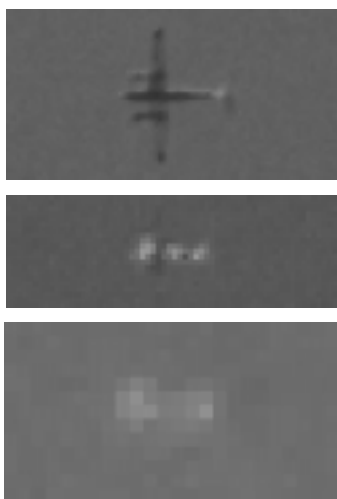


Figure 3. KingAir on three flight levels:  
Top: 1000m, middle line,  
Middle: 2000m, right line,  
Bottom: 4000m, left line

The DGPS data of the airplane was processed with the kinematic GPS software “GPSKIN” of IGP-GGL. An own ground reference station was set up at Zeughaus, Mels. In addition, the 1s data of three operational GPS reference stations (ETH Zürich, Davos, Pfänder) were used for the calculation of the airplane trajectories. The accuracy of the result was about the same for all reference stations; for the version with ETHZ which was finally used, the standard errors were 3.824 m in X-, 1.576 m in Y- and 2.332 m in Z-direction. This showed that the distance of about 100km to ETHZ, Davos and Pfänder is not too large as reference station distance.

The DGPS antenna of the airplane was manually measured in every image. From the exact acquisition time of the image, the position of the point could be determined from the GPS calculations. Figure 3 shows the plane at three different heights. Especially at higher altitudes, also due to the oblique viewing angle, the recognition of the plane and even more of the position of the antenna was very difficult. A set of independent manual measurements showed that the accuracy of the measurements are nevertheless  $\pm 1$  pixel for the middle line and  $\pm 2$  pixels for the left and right lines.

With a bundle adjustment (with fixed inner orientation parameters), the exterior orientation parameters were estimated for each camera. The image residuals show an accuracy of  $< 3$  pixel across-track which is consistent with the manual measurement accuracy, but an accuracy of 10-15 pixels along-track which is caused by the error in the precise acquisition time. At a mean velocity of the KingAir of 100m/s, 10 pixels correspond to a time error of about 100ms at the mean flight height. This accuracy is about the maximum, which can be achieved with our laptop system. For future calibrations with airplane flights, a more precise shutter release control should be considered. In addition, the GCP pointing accuracy distribution has to be improved with flight lines in both x- and y-direction instead of flight lines only parallel to the baseline. The stability of the angles in the bundle adjustment was improved with tie points on clouds near the image edges.

## 4.3 Exterior Orientation from Stars

As an alternative method to determine the exterior orientation angles and to have a validation of the airplane calibration, a method with star images was used. This method is also more realistic for an operational sky imager network where recalibration is necessary at regular time intervals. During clear nights, sky images with long exposure times were taken. The longest exposure time which can be set automatically with this camera type is 30 seconds. Longer exposure times have to be taken manually and are sometimes randomly interrupted after a few minutes. When the exposure time is longer than about one minute, the paths of the brightest stars can be seen between the noise. Although the noise represents a sum of dark current noise and sky background (atmospheric scatter light, etc.), it can be modelled to a large

extent by a dark current noise image, taken with a similar exposure time (Fig. 4). For the subtraction of the dark current noise (Fig. 4 right) from the star image (Fig. 4 left), the raw 8-bit camera files before any colour interpolation are used.

The enhanced star paths image is then further processed by a specialized software (Schildknecht, 1994) to identify the

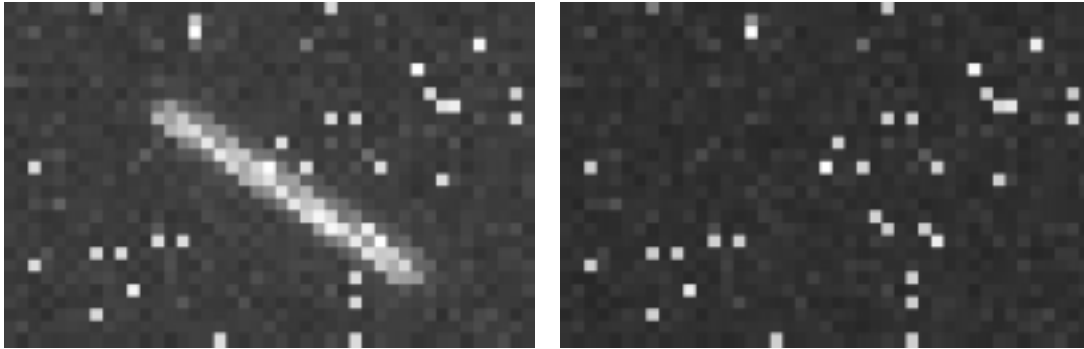


Figure 4. Left: star path and dark current noise, right: dark current noise

stars corresponding to the PPM (position and proper motion) star catalog. From the star positions, the orientation angles and the interior orientation parameters of both cameras were calculated with the same software package.

The optimal exposure time is based on two factors:

- Detectability of the linear feature within noise pattern: increases with increasing exposure time
- Linear form of star path: decreases with increasing exposure time

The star path is assumed to be a straight line by the processing software which finds the central point of each path by a centroid operator. Only these central points are used afterwards in the calculations. The best accuracy was achieved with this camera and lens type with an exposure time of 90 seconds.

#### 4.4 Comparison of orientation parameters

Inner and outer orientation parameters were very important not just for accurate 3-D point determination, but also because this known information should be used in matching to constrain the search along epipolar lines (Baltsavias, 1991). Since our matching program can not directly import all additional parameters estimated in the testfield calibration, also a version of the latter with only camera constant and principal point corrections was estimated. Both inner orientation values (termed withAP and noAP) were used in the orientation estimation with the aircraft resulting in different values for the rotation angles. In addition, a third set of values for orientation angles, camera constant and principal point was delivered from the orientation with the stars. The three datasets, especially withAp and stars, had a quite good fit with respect to inner orientation. However, the differences in the angles were large, reaching for kappa even more than one degree. To check the quality of inner and exterior orientation, well-defined points over the whole image format were selected in the left image and the distance of the epipolar lines from the true, manually measured corresponding points in the right image was calculated. Our expectation was that the rotation angles from stars would be the most accurate. However, with this orientation, the epipolar lines were misplaced in y up to 30 pixels. The best results were achieved with the inner orientation values of version withAP and the respective exterior orientation determination using the aircraft (maximum epipolar line displacement of 4 pixels). This orientation was further used in matching with a reduced weight for the geometric constraints, to allow finding corresponding points a few pixels away from the epipolar line.

Apart from errors in orientation angle determination, possible instabilities of the inner orientation of the DCS460 may have contributed these inconsistencies. In future applications, a stable camera will be used, testfield calibration for the inner orientation, use of all these parameters in matching, angle determination by using stars with the possibility to either adopt the inner orientation from the testfield calibration, or determine it and compare it to testfield calibration for detection of temporal changes.

## 5 CALCULATION OF CLOUD-BASE HEIGHT

### 5.1 Preprocessing

For the matching, the red channel, 8-bit, was used because of its better contrast (Fig. 5). The images are contrast-enhanced and radiometrically equalized with a Wallis filter (Wallis, 1976) (Fig. 6).

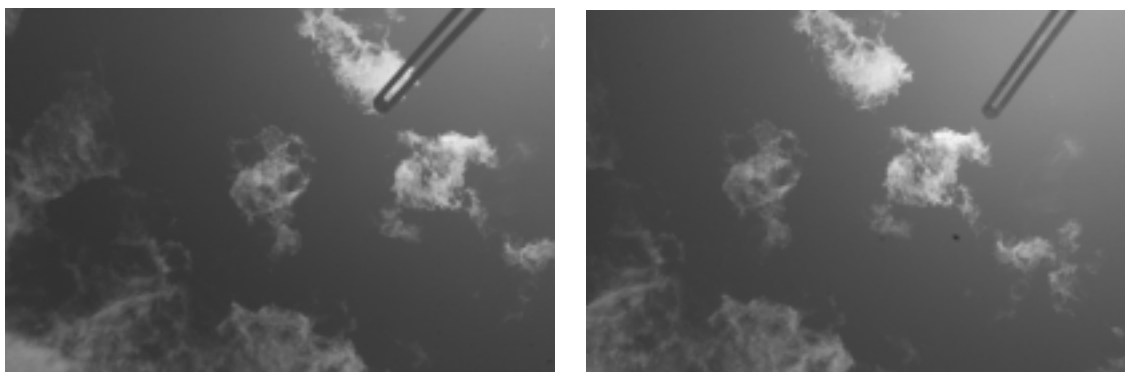


Figure 5. Stereo pair from ground-based cameras. a) left: Zeughaus, Mels b) right: Wiftech AG, Mels. A part of the sun occulter is seen at the top right.

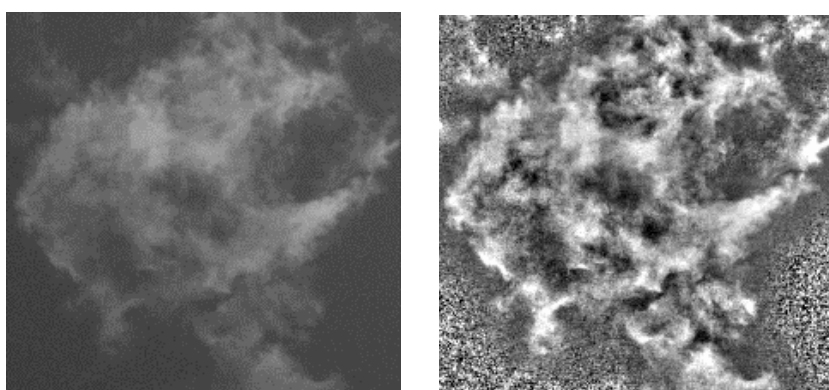


Figure 6. Left: Zoom of original image, right: same enhanced with a Wallis filter

## 5.2 Matching

### 5.2.1 Multiphoto Geometrically Constrained Matching

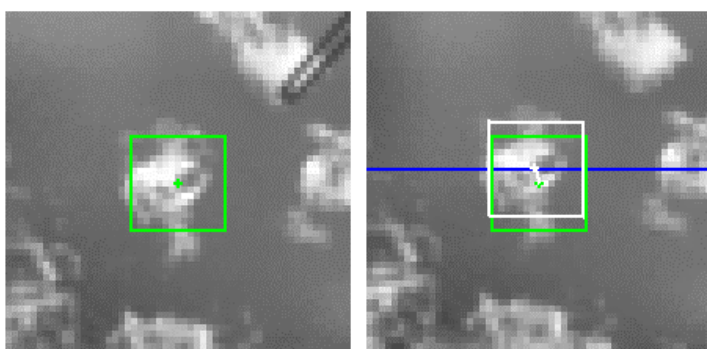


Figure 7. Constrained matching. Blue: epipolar line, green: initial value, white: matching solution.

With the geometric constraints, the search space is restricted to a region along the epipolar line. With our camera setup, the epipolar lines are horizontal in the images so that distinct points at non-horizontal edges should be selected for the matching (Fig. 7). The points along edges with angles of  $90^\circ \pm 80^\circ$  are found with the Foerstner operator.

Table 3 shows the result of three selected stereo pairs: an altocumulus and two cirrus situations. The cases were chosen with respect to the MAP validation data available.

Date, Time	Mean cloud height lowest layer [km]	Cloud height range lowest layer [m]	Mean cloud height second layer [km]	Cloud height range second layer [m]
08/10/1999, 10:58	4.0	3856 - 4173	-	-
13/10/1999, 10:16	8.0	7864 - 8089	10.9	10750 - 11046
20/10/1999, 09:37	10.8	9251 - 11980	-	-

Table 3. Results from the ground-based imager system for three selected cases (heights above sea-level).

### 5.2.2 Commercial Matching Software (VirtuoZo, Match-T)

Two commercial digital photogrammetric systems (VirtuoZo and Match-T) were tested for automatic derivation of CBH using matching. The inner and exterior orientation, as well as the affine transformation from pixel to photo coordinates were imported, albeit after a lot of effort to find out how to perform this, due to the very poor software documentation, especially with VirtuoZo. Both systems are tuned rather for aerial imagery and not CCD cameras without fiducial marks, but we finally managed to import the images and their information and try different matching

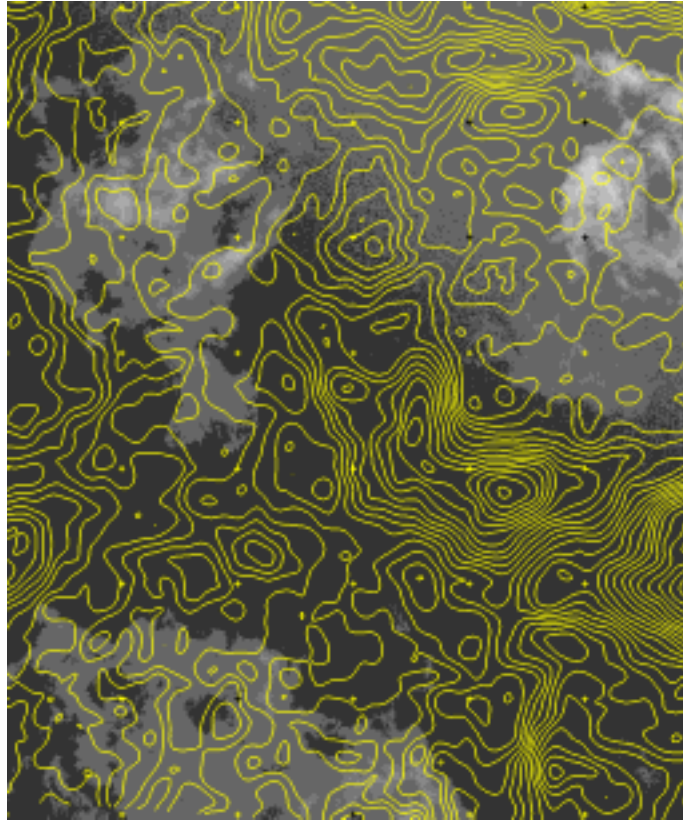


Fig. 8. Overlaid 20 m contours generated automatically with VirtuoZo.

versions. Match-T is based on an interest operator finding points with good texture, and found points everywhere in the image, even in pure blue sky. Clouds were modelled as bumps but not nicely and noncloud regions did not fall abruptly enough. VirtuoZo (especially an undulating matching strategy) performed better and at a fraction of the processing time. Fig. 8 shows contours with 20 m interval overlaid on the left image (08/10/1999 dataset). The average scale for this pair was 1:220,000 and the pixel footprint ca. 2 m. 10700 points with an average spacing of 30 m were matched automatically, resulting in a height range of 3720 - 4380 m. Even with VirtuoZo the results were not good enough, especially with low texture, thin clouds, not well-defined cloud edges etc. Thus, in future work we will adopt our own software to matching of cloud scenes.

## 6 VALIDATION OF THE RESULTS WITH COINCIDENT MAP MEASUREMENTS

A special composite observing system for the MAP-SOP was set up at the region of the Rhine Valley. Fig. 9 shows the location of our two cameras and of the lidar, radiosonde and surface climate stations which can be used for data comparison. Most of the systems were operated more or less continuously during the whole SOP; some were only switched on during IOPs.

### 6.1 Eye-observations

Eye-observations of the current weather situation including estimation of cloud parameters (cloud amount, cloud depth, cloud type(s), cloud-base height(s)) are performed 3-hourly at the main automatic climate stations, 4-hourly at the aero stations and 6-hourly at all other climate stations of the Swiss Meteorological Institute (SMI). It is important to note that these observations are sometimes done by different persons at the same station so that the subjectivity of the estimated values is not only between stations but also within the time series of one station. The data of the automatic stations Chur and Vaduz, the climate station Bad Ragaz and the aero station Weesen were taken as comparison for the 08/10/1999

09:30 and 13/10/1999 10:15 case. On 08/10/1999, all stations reported a cloud amount between 1/8 and 3/8; the cloud type and height at Chur was cirrus with an estimated height of 5.1 to 7.0 km; at Weesen, altocumulus with a height of about 3 km above ground was observed. At 06:00, altocumulus with an approximated height of 4.5 km was reported at Chur. These observations are consistent with our images and results of altocumulus with a height range between 3.4 and 3.7 km. On 13/10/1999, Weesen and Vaduz reported fog; the cloud amount at Bad Ragaz and Chur was between 1/8 and 6/8 (06:00 – 12:00) and the type cirrus with a height range between 7.2 and 9.0 km. This case does fit with the lower clouds in our images but not with the higher layer. The estimation of cirrus cloud-base heights from ground eye-observations is nearly impossible and the height is underestimated in most cases.

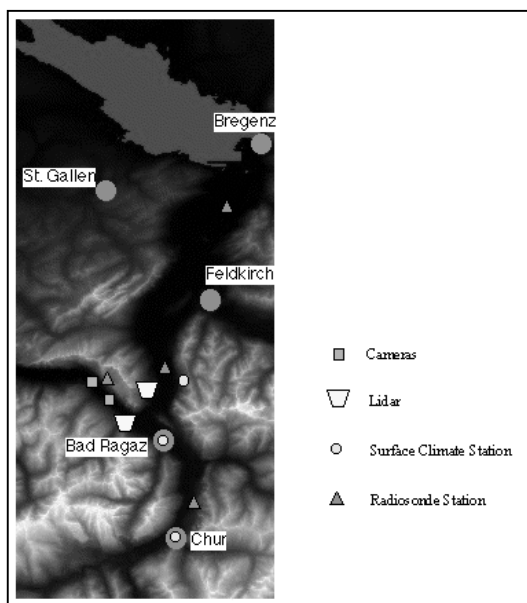


Figure 9. Stations which measured cloud-base heights during MAP

## 6.2 Lidar

A first comparison was done with the data of the Pseudo-Random Noise modulation, continuous wave (PRN-cw) total backscatter lidar of the Observatoire de Neuchâtel (Matthey et al., 1996) which was located at Trübbach. This prototype lidar was in operation mainly during MAP-IOPs (Intensive Observation Periods). The lidar signal of the 20/10/1999 case is unfortunately very weak due to the large height of the clouds; varying peak signals at 10.2, 10.7, 10.8, 11.0, 11.1 and 11.4 km above ground are found between 09:00 and 09:45 (Frioud, personal communication). Although there is a

correspondance between the imager and lidar values, further cases with lower clouds will have to be analyzed where the lidar signals are strong enough to determine distinct cloud layers.

## 6.3 Radiosondes

7 temporary radiosonde stations were operated by the Swiss Army during the MAP-SOP in the greater Rhine Valley area. They consist of two types of sondes:

- Low-level sondes, measuring temperature and wind.
- High-level sondes, measuring pressure, temperature, humidity and wind.

A method for estimating cloud-base heights from radiosonde data is described in (Chernykh and Eskridge, 1996). In the sounding launched at 11:00 UTC at Diepoldsau, the lowest cloud layer can be well defined from about 630 to 600 hPa which corresponds to a height of 3.9 to 4.4 km above sea-level. The temperature profiles of the low-level stations Heiligkreuz and Buchs show the same shape. The results from the ground-based stereo images correspond therefore very well with the lowest cloud layer values from these soundings.

## 6.4 ATSR2 CTH (for vertically thin clouds)

Cloud-top heights from ATSR2 satellite images are calculated for 13/10/1999 10:18 with the method described in (Poli et al., 2000). The field of view of the ground-based imager corresponds to only about 14 x 9 ATSR2 pixels. The retrieved mean height in this area is 12.0 km above sea-level from the 11 $\mu$ m channel and 13.0 km from the 0.87  $\mu$ m channel. The matching of the cirrus clouds in this area was much more accurate with the 11 $\mu$ m channel (less blunders). This case shows the possibility of coincident ground- and satellite-based stereo analysis of clouds and of the validation of satellite-based cloud-top heights of vertically thin clouds with ground-based imagers.

## 7 CONCLUSIONS

The measurements with the developed ground-based cloud imager during the MAP-SOP have shown the capacity of this system to determine the cloud-base height. The accurate calibration and sensor orientation are very important for an efficient use in our geometrically constrained matching program. The method with star calibration of the orientation angles, GPS measurement of the camera positions and the testfield calibration for the interior orientation parameters seems to be a realistic and also operationally usable method. The time acquisition duration of the star images should be changed to about 90 seconds. The potential of the airplane calibration could be used for a control of the consistency of

the various orientation parameters. A new sensor will be selected where the stability of the CCD chip can be ensured over a longer time period.

For the constrained matching, selection of match points by an appropriate interest operator, making also use of image-derived cloud masks will be performed. Derivation of approximations by feature-based matching and/or starting from a lower pyramid level, will allow a better modelling of the cloud and its boundaries and avoiding bridging over variable objects (clouds and sky, clouds of different height) through the current use of area patches. More than 2 cameras would expand the number of points which can be used in the matching and would stabilize the matching in the self-similar texture of clouds, especially if the approximation of the initial values is not very good.

Further cloud parameters like cloud amount and cloud-base motion will be extracted from the data.

## ACKNOWLEDGEMENTS

The MAP data was provided by the various principal investigators of the MAP Rhine Valley target area and the Swiss Meteorological Institute. We thank Marc Cocard, ETH-GGL, for the GPS software and support, the Astronomical Institute Berne for the star processing, the Swiss Army for the calibration flights, Kodak and FHBB Muttentz for providing the DCS460 cameras and Maria Pateraki for the tests with the commercial matching software. This work is funded by the Bundesamt für Bildung und Wissenschaft (BBW) within the EU-project CLOUDMAP (BBW Nr. 97.0370).

## REFERENCES

- Adams, J.E. Jr, Parulski, K., Spaulding, K., 1998. Color Processing in Digital Cameras. *IEEE Micro*, 18(6), pp. 20-30.
- Allmen, M.C., Kegelmeyer jr., W.Ph., 1996. The computation of cloud-base height from paired whole-sky imaging cameras. *J. Atmos. Ocean. Techn.*, 13(2), pp. 97-113.
- Baltsavias, E.P., 1991. Multiphoto Geometrically Constrained Matching. Ph. D. dissertation, Institute of Geodesy and Photogrammetry, ETH Zurich, Mitteilungen No. 49, 221 p.
- Bayer, B.E., 1976. Color imaging array. United States Patent 3,971,065, US Patent and Trademark Office, Washington, DC, USA.
- Beyer, H.A., 1992. Geometric and radiometric analysis of a CCD-camera based photogrammetric close-range system. Ph.D. dissertation, Institute of Geodesy and Photogrammetry, ETH Zurich, Mitteilungen No. 51, 186 p.
- Brown, D.C., 1971. Close-range camera calibration. *Photogrammetric Engineering*, 37(8), pp. 855-866.
- Chernykh, I.V., Eskridge, R.E., 1996. Determination of cloud amount and level from radiosonde soundings. *J. Appl. Met.*, 35(8), pp. 1362-1369.
- MAP Implementation Plan, 1999. <http://www.map.ethz.ch/SOPprep.htm> (accessed March 30, 2000).
- MAP Science Plan, 1998. <http://www.map.ethz.ch/splan/spindex.htm> (accessed March 30, 2000).
- Matthey, R., Mitev, V., Weibel, P., 1996. PRN-cw backscatter lidar measurements with a powerful narrowband diode laser. In: Ansmann, A., Neuber, R., Rairoux, P., Wandinger, U. (Eds.), *Advances in atmospheric remote sensing with lidar*.
- Poli, D., Seiz, G., Baltsavias, E.P., 2000. Cloud-top height estimation from satellite stereopairs for weather forecasting and climate change analysis. In: *IAPRS, Vol. 33 (proc. of this Congress)*.
- Schildknecht, Th., 1994. Optical astrometry of fast moving objects using CCD detectors. Ph. D. dissertation. Astronomical Institute, University of Berne. *Geodätisch-geophysikalische Arbeiten in der Schweiz*, Vol. 49.
- Shields, J.E., Karr, M.E., Tooman, T.P., Sowle, D.H., Moore, S.T., 1999. The whole sky imager – a year of progress. [http://www-mpl.ucsd.edu/people/jshields/shields\\_98.pdf](http://www-mpl.ucsd.edu/people/jshields/shields_98.pdf) (accessed March 30, 2000).
- Shortis, M.R., Robson, S., Beyer, H.A., 1998. Principal point behaviour and calibration parameter models for Kodak DCS cameras. *Photogrammetric Record*, 16(92), pp. 165-186.
- Stokes, G.M., Schwartz, S.E., 1994. The Atmospheric Radiation Measurement (ARM) Program: Programmatic background and design of the cloud and radiation test bed. *Bull. Am. Met. Soc.*, 75(7), pp. 1201-1221.
- Wallis, R., 1976. An approach to the space variant restoration and enhancement of images. *Proc. of Symp. on Current Mathematical Problems in Image Science*, Naval Postgraduate School, Monterey CA, USA, November.